Short Communication

MUC1 traverses apical recycling endosomes along the biosynthetic pathway in polarized MDCK cells

Polly E. Mattila[1,a], Carol L. Kinlough[1,a], Jennifer R. Bruns[1], Ora A. Weisz[1,2] and Rebecca P. Hughey[1,2,*]

[1] Department of Medicine, Renal-Electrolyte Division, University of Pittsburgh School of Medicine, Pittsburgh, PA 15261, USA

[2] Department of Cell Biology and Physiology, University of Pittsburgh School of Medicine, Pittsburgh, PA 15261, USA

*Corresponding author
e-mail: hugheyr@pitt.edu

Abstract

MUC1 is a heavily glycosylated transmembrane protein localized at the apical surface of polarized epithelial cells. Here, we examined the biosynthetic route of newly synthesized MUC1 in polarized Madin-Darby canine kidney (MDCK) cells. Apically and basolaterally destined cargo are sorted at the *trans*-Golgi network into distinct vesicles, and proteins with lipid raft-dependent apical targeting signals and glycan-dependent apical targeting signals appear to specifically transit apical early endosomes (AEEs) and apical recycling endosomes (AREs), respectively. Using metabolic labeling we found that MUC1 is efficiently targeted to the apical surface of polarized MDCK cells with a $t_{1/2}$ of 45 min. Apical delivery was not altered by inactivation of AEEs by treatment with hydrogen peroxide and diaminobenzidine treatment after apical loading of endosomes with horseradish peroxidase-conjugated wheat germ agglutinin. However, expression of a GFP-tagged myosin Vb tail fragment (GFP-MyoVbT) that disrupts export from the ARE significantly reduced MUC1 apical expression. Moreover, MUC1 expressed for brief periods in MDCK cells co-localized with GFP-MyoVbT. We conclude that MUC1 traffics to the apical surface via AREs in polarized renal epithelial cells.

Keywords: apical; biosynthetic traffic; endosome; glycosylation; Madin-Darby canine kidney (MDCK); MUC1; myosin Vb; polarity.

MUC1 is a transmembrane glycoprotein localized to microvilli on the apical surface of polarized epithelial cells. The heavily glycosylated ectodomain of MUC1 yields protection from pathogens by providing binding sites for bacteria and viruses (Muller et al., 1997; Lillehoj et al., 2002), while its comparatively small cytoplasmic tail exhibits numerous sites for protein docking, phosphorylation and palmitoylation that regulate signal transduction as well as MUC1 endocytosis and recycling (Kinlough et al., 2004, 2006; Singh and Hollingsworth, 2006; Hattrup and Gendler, 2008). While the ectodomain can be shed from the cell surface after proteolysis, the cytoplasmic tail is found under various physiological conditions in either the cytoplasm, nucleus or mitochondria, where it modulates adherens junctions, transcription of some target genes, and apoptosis, respectively (Brayman et al., 2004; Singh and Hollingsworth, 2006). In non-polarized tumor cells, MUC1 is a substrate for the EGF receptor kinase and clearly functions as a modifier of EGF receptor membrane trafficking and its downstream signaling (Li et al., 2001; Pochampalli et al., 2006). The expression of mouse MUC1 during embryogenesis is restricted to the apical surfaces of secretory epithelial cells and correlates with epithelial differentiation (Braga et al., 1992). MUC1 is expressed in both the collecting ducts and distal tubules in both humans (Zotter et al., 1988) and in transgenic mice expressing human MUC1 in the absence of mouse Muc1 (Peat et al., 1992). Although MUC1 is not found in the normal proximal tubule in the adult, MUC1 is present on the apical surface of the tubule after acute renal damage consistent with dedifferentiation of the cells and a role for MUC1 in repair of epithelia (Howie, 1986; Braga et al., 1992).

MUC1 is synthesized as a single peptide that undergoes autocatalytic cleavage to yield a stable heterodimer (Ligtenberg et al., 1992; Parry et al., 2001; Macao et al., 2006). The small transmembrane subunit contains one site for N-linked glycosylation, and modification of this consensus site closest to the transmembrane domain is required for galectin-3 binding and thereby physical and functional interaction with the EGF receptor (Ramasamy et al., 2007). The large subunit has four sites for N-linked glycosylation and a variable number of near-perfect 20-residue tandem repeats, each with five potential sites for O-linked glycosylation (Hanisch and Muller, 2000). MUC1 is internalized from the cell surface by clathrin-mediated endocytosis and is efficiently recycled (Altschuler et al., 2000; Kinlough et al., 2004, 2006). Interestingly, comparison of glycan structures on transmembrane and an anchor-minus secreted variant of MUC1 indicates that transmembrane MUC1 is further modified upon recycling to increase its sialylation and its content of core 1 O-linked glycans (Litvinov and Hilkens, 1993; Engelmann et al., 2005).

We are interested in the signals and pathways that direct newly synthesized MUC1 to the apical surface of renal epithelial cells. Apical targeting of proteins can be

---

[a] These authors contributed equally to this work.

mediated by a variety of sorting signals, including cytosolic or transmembrane peptide motifs, glycosylphosphatidylinositol (GPI) linkages, and N-linked or O-linked glycosylation (for review, see Potter et al., 2006). Newly synthesized transmembrane and secretory proteins are co-translationally translocated into the lumen of the endoplasmic reticulum (ER) and concurrently modified with core N-linked oligosaccharides. Loss of terminal sugars on N-glycans occurs during glycoprotein folding within the ER, as the processed glycans are key for interaction with some chaperones and several components of the ER quality control pathway (Christianson et al., 2008; Nakatsukasa and Brodsky, 2008). Properly folded proteins are subsequently exported to the Golgi complex, where terminal processing of both N-linked and O-linked glycans continues. Sorting of apically and basolaterally destined proteins into distinct transport carriers is thought to occur in the distal compartment of the Golgi complex termed the *trans*-Golgi network (TGN). Additionally, proteins that contain different types of apical sorting signals are apparently sorted into separate subpopulations of vesicles that bud from the TGN (Jacob and Naim, 2001; Polishchuk et al., 2004; Guerriero et al., 2006, 2008).

Further complexity in the biosynthetic trafficking routes of apically destined proteins in polarized renal epithelial cells has emerged in recent studies. Rather than trafficking directly from the TGN to the plasma membrane surface, many newly synthesized proteins appear to traverse endosomal compartments prior to reaching the apical surface. In particular, a distinction has emerged between the pathways used by proteins that have glycosylation-dependent and glycosylation-independent apical targeting signals (Cresawn et al., 2007). For example, apical delivery of endolyn, a sialomucin whose apical targeting is mediated by two of its eight N-glycans, was found to involve transient passage through the apical recycling endosome (ARE) in polarized Madin-Darby canine kidney (MDCK) cells. The ARE is a subapical compartment 'marked' by the small G protein Rab11 and the motor protein myosin Vb. Expression of a dominant-negative mutant encoding a GFP-tagged tail fragment of myosin Vb (GFP-MyoVbT) inhibited apical delivery of newly synthesized endolyn to the apical surface. Moreover, endolyn staged along the biosynthetic pathway was observed to co-localize in the ARE with Rab11 and GFP-MyoVbT (Cresawn et al., 2007). In contrast, proteins targeted to the apical surface by signals within their transmembrane domains or by GPI anchors were unaffected by expression of the myosin Vb tail (Cresawn et al., 2007). These latter apical proteins share the common distinction of being partially insoluble in cold detergent, a feature of proteins affiliated with glycolipid-enriched microdomains or lipid rafts. Interestingly, apical delivery of these raft-associated proteins also appears to involve passage through an apical endocytic compartment distinct from the ARE. Apical internalization of wheat germ agglutinin conjugated to horseradish peroxidase (HRP-WGA) followed by subsequent HRP-mediated crosslinking and inactivation/ablation of accessible compartments resulted in the selective inhibition in delivery of newly synthesized raft-associated proteins, such as influenza hemagglutinin (HA), but had no effect on endolyn traffic to the apical surface (Cresawn et al., 2007). Based on immunofluorescence studies demonstrating efficient co-localization of apically internalized fluorescently tagged WGA (FITC-WGA) with the early endosomal marker EEA1, we concluded that lipid raft-associated proteins traffic through apical early endosomes (AEEs) (Cresawn et al., 2007). Thus, glycosylation-dependent and lipid raft-dependent apical targeting mechanisms may direct proteins to the apical surface via distinct trafficking routes.

The apical targeting signal for MUC1 has not yet been defined, but clearly resides in the heavily glycosylated ectodomain. Pemberton et al. (1996) observed that a chimera of the MUC1 ectodomain attached to the transmembrane and cytoplasmic domains of a basolaterally expressed protein CD2 was apically expressed in MDCK cells. Consistent with a role for terminal processing of glycans in surface expression of MUC1, Huet et al. (1998) observed intracellular accumulation of MUC1 in HT-29 colon carcinoma cells treated with benzyl-GalNAc, which inhibits sialylation of both N-linked and O-linked glycans. Moreover, MUC1 expressed in MDCK cells is largely soluble in cold Triton X-100, suggesting that it is not associated with lipid rafts (Kinlough et al., 2006). Thus, we hypothesized that newly synthesized MUC1 might traffic to the apical surface of polarized MDCK cells via the ARE as observed for endolyn. To test this, we examined delivery of newly synthesized MUC1 to the apical cell surface in MDCK cells after either (i) ablation of AEEs with HRP-WGA-dependent crosslinking, or (ii) a block of membrane trafficking through AREs by expression of the myosin Vb tail.

To study MUC1 trafficking in polarized MDCK cells, we prepared a replication-defective recombinant adenovirus encoding MUC1 (AV-MUC1) and used it to infect MDCK-T23 cells cultured on permeable supports for 3 days (Figure 1A). The next day, the infected cells were metabolically radiolabeled for 20 min with [^{35}S]Met/Cys and chased up to 2 h before treatment of the apical or basolateral surface with the membrane impermeant biotinylating reagent sulfo-NHS-SS-biotin. Analysis of the biotinylated [^{35}S]MUC1 recovered with avidin-conjugated beads from immunoprecipitates revealed that MUC1 was efficiently delivered to the apical surface with a $t_{1/2}$ of approximately 45 min, similar to the kinetics of surface delivery in non-polarized CHO cells (Kinlough et al., 2006). The kinetics of MUC1 polarized delivery in AV-MUC1 infected MDCK-T23 were identical to those observed for MUC1 in a clone of MDCK cells stably transfected with pcDNA3-MUC1, and the combined data from three experiments are presented in Figure 1B. A small fraction of newly synthesized MUC1 also appeared on the basolateral surface but mostly disappeared by 120 min chase, when >90% of surface MUC1 was apically localized. Transient basolateral delivery of other newly synthesized apical proteins has previously been observed (Casanova et al., 1991). The distribution of newly synthesized MUC1 after 120 min chase was similar to steady-state MUC1 polarity determined by immunoblotting (data not shown).

We previously observed that apical biosynthetic delivery of the raft-associated protein HA, but not the
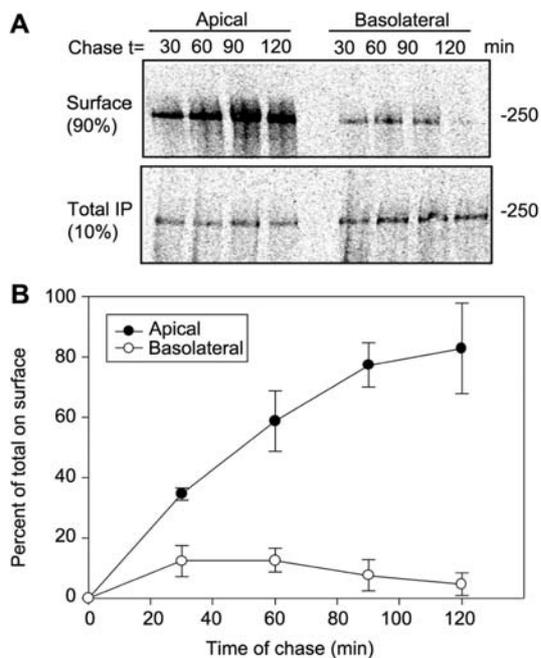
Figure 1 Newly synthesized MUC1 is targeted to the apical surface of polarized MDCK cells.

AV-MUC1 was generated by subcloning cDNA for MUC1 with 22 tandem repeats (M_r 250 000) into the pAdlox vector using standard techniques (Hardy et al., 1997). MDCK-T23 cells stably express the tetracycline-repressible transactivating protein required for suppression of specified promoters (see legend of Figure 2), and were used for all experiments in this manuscript unless noted otherwise. Polarized MDCK-T23 cells were infected 3 days after plating on Costar permeable supports (Corning, NY, USA) with AV-MUC1 at a multiplicity of infection (m.o.i.) of 100. On day 4, cells were starved for 30 min in medium lacking Met and Cys, pulse-labeled for 20 min with [^{35}S]Met/Cys, and chased in normal culture medium for up to 2 h prior to biotinylation of the apical or basolateral surface as previously described (Kinlough et al., 2006; Cresawn et al., 2007). Cells were extracted in detergent and surface-biotinylated MUC1 was recovered with avidin-conjugated beads after immunoprecipitation with mouse monoclonal antibody B27.29 (Fujirebio Diagnostics, Inc., Malvern, PA, USA). Aliquots of total immunoprecipitate (Total IP, 10%) and biotinylated MUC1 (Surface, 90%) were subjected to SDS-PAGE on Criterion precast 4–15% gradient gels (Bio-Rad, Hercules, CA, USA). The gel was dried and the radiolabeled MUC1 was analyzed with a Bio-Rad Personal Imager. A representative gel profile is shown in panel (A). As the kinetics of MUC1 delivery were identical in MDCK-T23 cells infected with AV-MUC1 and in MDCK cells stably transfected with MUC1, data were combined from experiments with single time points, and the percent of total cellular [^{35}S]MUC1 found on the apical or basolateral surface during the chase period is presented in panel (B) as mean and SD (n=3). Mobility of Bio-Rad Precision Plus Protein All Blue standards (denoted as molecular mass× 10^{-3}) is indicated on the right of the gels.

non-raft associated marker endolyn, was inhibited by inactivation of AEE accessible to apically internalized HRP-WGA (Cresawn et al., 2007). FITC-WGA internalized for 15 min at 37°C co-localized largely with the early endosomal marker EEA1 and did not localize with furin or Rab11, markers of the TGN and ARE, respectively (Cresawn et al., 2007). We used the same experimental protocol to determine if MUC1 transits AEEs. Polarized MDCK cells infected with AV-MUC1 were pulse labeled for 15 min with [^{35}S]Met/Cys at 37°C, and then incubated

for 1 h at 19°C with or without HRP-WGA in the apical medium. After internalization of HRP-WGA, remaining surface HRP-WGA was stripped by incubating the cells with 0.1 M GlcNAc. To inactivate the AEE pre-loaded with HRP-WGA, cells were incubated on ice for 1 h with 3,3′-diaminobenzidine tetrahydrochloride and hydrogen peroxide. Cells were subsequently chased for 45 min at 37°C prior to determination of apical surface delivery by surface biotinylation as described for Figure 1. Comparison of the apical MUC1 in cells incubated with or without HRP-WGA revealed that biosynthetic delivery of MUC1 to the apical surface was not altered by ablation of AEEs (27.9%±6.9 with HRP-WGA and 26.0%±7.2 without HRP-WGA; $p>0.5$ by Student's t-test, n=5–6). In contrast, delivery of HA to the apical surface of AV-HA infected MDCK cells (measured in parallel samples by surface trypsin treatment in the same experiments) was significantly reduced by AEE ablation (42.3%±2.3 with HRP-WGA vs. 38.9%±2.4 in control cells; $p<0.05$ by Student's t-test, n=6). We note that in this series of experiments, the effect of AEE ablation on HA delivery, though statistically significant, was more modest than we previously observed (Cresawn et al., 2007). Based on these data, we cautiously interpret these results to suggest that MUC1 does not transit the AEE along the biosynthetic pathway.

We previously found that endolyn (but not HA) delivery to the apical surface of MDCK-T23 cells was blocked by expression of GFP-MyoVbT, which localizes to the ARE and inhibits export of transcytosing and apical recycling cargo from this compartment (Biscardi et al., 1999). To examine the effect of ARE perturbation on MUC1 apical delivery, polarized parental MDCK-T23 cells and two independent mixed populations of GFP-MyoVbT-expressing cells were infected with AV-MUC1 or with an adenovirus encoding endolyn as a positive control (Figure 2). The following day, cells were pulse labeled for 30 min with [^{35}S]Met/Cys and chased for 2 h prior to biotinylation of the apical or basolateral surface. Comparison of the fraction of surface MUC1 between variously treated groups revealed that biosynthetic delivery of MUC1 to the apical surface was significantly reduced by perturbation of the ARE. As we previously observed, biosynthetic delivery of endolyn was also significantly reduced.

We next asked whether we could visualize newly synthesized MUC1 in the GFP-MyoVbT-positive compartment. As we previously reported that a chimera of MUC1 transmembrane and cytoplasmic domains attached to Tac ectodomain (Tac-MUC1) was directed to recycling endosomes in CHO cells (Kinlough et al., 2006), it was essential to avoid post-endocytic trafficking of MUC1 while trying to visualize the biosynthetic trafficking of MUC1. To this end, we expressed MUC1 in cells for a brief period after infection with AV-MUC1, and then chilled the cells to 19°C to accumulate an intracellular pool of newly synthesized protein in the TGN with minimal delivery to the cell surface. We were unable to find infection and staging conditions that allowed us to detect a biosynthetic pool of MUC1 in fully polarized cells without the accumulation of significant levels of MUC1 at the cell surface. However, we were able to obtain satisfactory
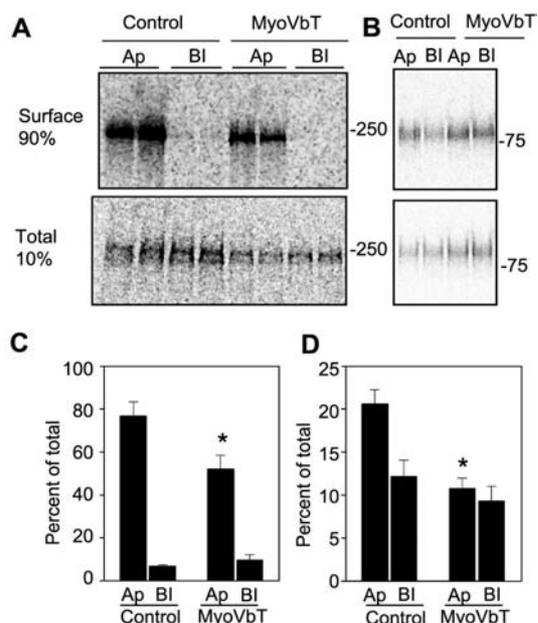
Figure 2 Apical biosynthetic delivery of MUC1 is disrupted in cells expressing the myosin Vb tail.
Mixed populations of MDCK-T23 cells stably expressing a tetracycline-repressible GFP-tagged myosin Vb tail (MyoVbT) and parental MDCK T23 cells were cultured on permeable supports for 3 days in the absence of tetracycline and then infected with AV-MUC1 (A and C) or AV-endolyn (B and D). The day after infection, cells were radiolabeled for 30 min with [^{35}S]Met and Cys for MUC1-infected cells and [^{35}S]Cys for endolyn-infected cells, and chased for 2 h prior to surface biotinylation as described previously and in the legend to Figure 1 (Kinlough et al., 2006; Cresawn et al., 2007). Representative gels for total immunoprecipitated (Total, 10%) and biotinylated (Surface, 90%) [^{35}S]MUC1 (A) or [^{35}S]endolyn (B) are shown. The fraction of total [^{35}S]MUC1 (C) or [^{35}S]endolyn (D) found on the apical or basolateral cell surface was calculated from multiple experiments (n=3, mean and SEM). By Student's t-test, the p-value (*) for MUC1 (C) and endolyn (D) apical surface expression between MyoVbT and control MDCK-T23 cells were <0.05 and <0.03, respectively. Mobility of Bio-Rad Precision Plus Protein All Blue standards (denoted as molecular mass×10^{-3}) is indicated on the right of the gels.

expression conditions using MCDK cells grown on coverslips, although non-polarized cells express only a single class of recycling endosome in which Rab11 and myosinVb co-localize with recycling transferrin. These cells were (i) infected for 1 h with AV-MUC1, (ii) allowed to express the protein for 2 h at 37°C, (iii) incubated at 19°C for 2 h to maximize accumulation of newly synthesized MUC1 in the TGN, and (iv) warmed to 37°C for 15 min. The cells were subsequently fixed and processed for indirect immunofluorescence to visualize MUC1 and GFP-MyoVbT. As a control, we also stained uninfected GFP-MyoVbT-expressing cells using anti-MUC1 antibody (Figure 3). We observed several bright punctate structures in these uninfected cells that presumably represent background staining. These structures were also present in AV-MUC1 infected cells, although clear expression of MUC1 was also visible. Most of the MUC1 staining was intracellular, as expected given the brief expression period, and there was obvious co-localization of a portion of the MUC1 staining with GFP-MyoVbT.

A model summarizing the apical trafficking routes of MUC1 and other apical markers is shown in Figure 4. Taken together, our studies suggest that newly synthesized MUC1 traffics through the ARE prior to reaching the apical membrane of polarized renal epithelial cells. Although the apical targeting signal in MUC1 is not known, the itinerary of MUC1 is similar to that of apical proteins with glycosylation-dependent sorting signals, such as endolyn. We found no effect of inactivating AEEs on apical delivery of MUC1, although in our experiments reported here the effect of this maneuver on delivery of our positive control (influenza HA), albeit statistically significant, was considerably less than we previously observed (Cresawn et al., 2007). Thus, we cannot formally exclude the possibility that a fraction of MUC1 transits through the AEE. However, this does not appear to be the case for endolyn, as we previously found that inactivating AEEs in cells expressing GFP-MyoVbT did not further reduce apical delivery of endolyn (Cresawn et al., 2007).
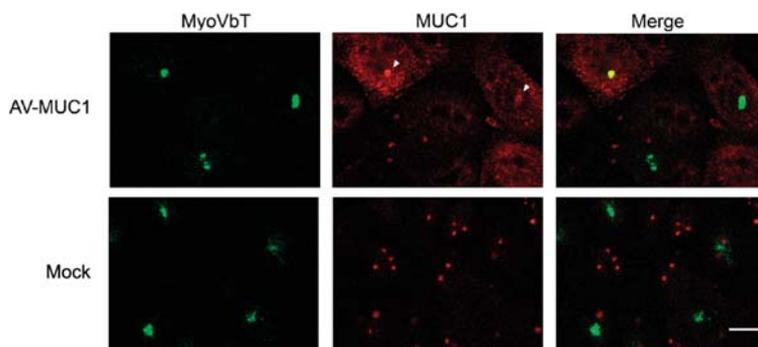

Figure 3 Newly synthesized MUC1 co-localizes with GFP-MyoVbT.
MDCK-T23 cells expressing GFP-tagged myosin Vb tail (MyoVbT) were infected for 1 h with AV-MUC1, then incubated for 2 h at 37°C to initiate MUC1 synthesis. The cells were then transferred to 19°C for 2 h in the presence of 50 μg/ml cycloheximide to accumulate newly synthesized protein in the *trans*-Golgi network, then warmed to 37°C for 15 min. Cells were fixed and processed for indirect immunofluorescence with anti-MUC1 monoclonal antibody B27.29 (top row). Mock-infected cells were treated and processed in parallel to visualize background antibody staining (bottom row). A fraction of MUC1 in expressing cells was observed in GFP-MyoVbT-positive compartments (arrowheads). Scale bar=10 μm.
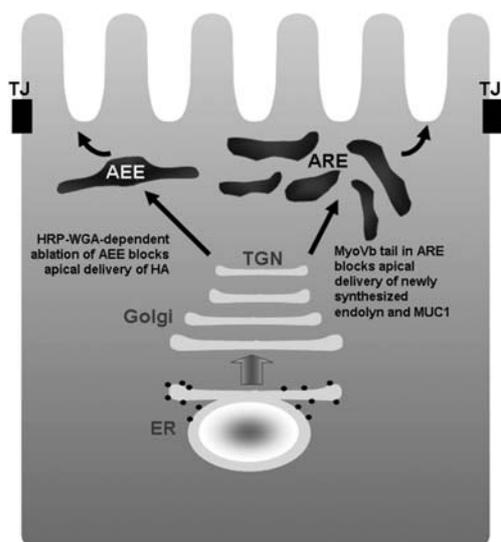
Figure 4 Biosynthetic delivery of apical proteins in polarized MDCK cells.
The indirect routes taken by newly synthesized raft-associated and glycan-dependent proteins are shown in this model of a polarized MDCK cell (TJ are tight junctions). HRP-WGA-mediated ablation of apical early endosomes (AEEs) blocks apical delivery of the lipid raft-associated protein HA, but has no effect on delivery of newly synthesized MUC1 or endolyn. Expression of the MyoVb tail fragment in the apical recycling endosome (ARE) blocks apical delivery of MUC1 and endolyn, but has no effect on HA.

What is the purpose of an indirect apical delivery route for MUC1? Given the importance of MUC1 during development and its many signaling functions, cells may need to carefully modulate surface MUC1 expression levels. This may be accomplished in part by funneling newly synthesized and recycling pools of MUC1 into a common compartment from which surface delivery can be fine-tuned. We previously reported that the cytoplasmic tail of MUC1 can direct a neutral reporter (Tac) to a Rab11-positive compartment after internalization in non-polarized CHO cells, and that palmitoylation of the Tac-MUC1 tail is required for its efficient exit from this compartment (Kinlough et al., 2006). It will be important to determine whether disruption of MUC1 palmitoylation sites also delays exit of newly synthesized MUC1 from Rab11 positive compartments in polarized MDCK cells.

Acknowledgments

References

Altschuler, Y., Kinlough, C.L., Poland, P.A., Bruns, J.B., Apodaca, G., Weisz, O.A., and Hughey, R.P. (2000). Clathrin mediated endocytosis of MUC1 is modulated by its glycosylation state. Mol. Biol. Cell 11, 819–831.

Biscardi, J.S., Maa, M.C., Tice, D.A., Cox, M.E., Leu, T.H., and Parsons, S.J. (1999). c-Src-mediated phosphorylation of the epidermal growth factor receptor on Tyr845 and Tyr1101 is associated with modulation of receptor function. J. Biol. Chem. 274, 8335–8343.

Braga, V.M.M., Pemberton, L.F., Duhig, T., and Gendler, S.J. (1992). Spatial and temporal expression of an epithelial mucin, Muc-1, during mouse development. Development 115, 427–437.

Brayman, M., Thathiah, A., and Carson, D.D. (2004). MUC1: a multifunctional cell surface component of reproductive tissue epithelia. Reprod. Biol. Endocrinol. 2, 4.

Casanova, J.E., Mishum, Y., Ikehara, Y., Hubbard, A.L., and Mostov, K. (1991). Direct apical sorting of rat liver dipeptidylpeptidase IV expressed in Madin-Darby Canine Kidney Cells. J. Biol. Chem. 266, 24428–24432.

Christianson, J.C., Shaler, T.A., Tyler, R.E., and Kopito, R.R. (2008). OS-9 and GRP94 deliver mutant α1-antitrypsin to the Hrd1-SEL1L ubiquitin ligase complex for ERAD. Nat. Cell Biol. 10, 272–282.

Cresawn, K.O., Potter, B.A., Oztan, A., Guerriero, C.J., Ihrke, G., Goldenring, J.R., Apodaca, G., and Weisz, O.A. (2007). Differential involvement of endocytic compartments in the biosynthetic traffic of apical proteins. EMBO J. 26, 3737–3748.

Engelmann, K., Kinlough, C.L., Muller, S., Razawi, H., Baldus, S.E., Hughey, R.P., and Hanisch, F.G. (2005). Transmembrane and secreted MUC1 probes show trafficking-dependent changes in O-glycan core profiles. Glycobiology 15, 1111–1124.

Guerriero, C.J., Weixel, K.M., Bruns, J.R., and Weisz, O.A. (2006). Phosphatidylinositol 5-kinase stimulates apical biosynthetic delivery via an Arp2/3-dependent mechanism. J. Biol. Chem. 281, 15376–15384.

Guerriero, C.J., Lai, Y., and Weisz, O.A. (2008). Differential sorting and Golgi export requirements for raft-associated and raft-independent apical proteins along the biosynthetic pathway. J. Biol. Chem. 283, 18040–18047.

Hanisch, F.-G. and Muller, S. (2000). MUC1: the polymorphic appearance of a human mucin. Glycobiology 10, 439–449.

Hardy, S., Kitamura, M., Harris-Stansil, T., Dai, Y., and Phipps, M.L. (1997). Construction of adenovirus vectors through Cre-lox recombination. J. Virol. 71, 1842–1849.

Hattrup, C.L. and Gendler, S.J. (2008). Structure and function of the cell surface (tethered) mucins. Annu. Rev. Physiol. 70, 431–457.

Howie, A.J. (1986). Epithelial membrane antigen in normal and proteinuric glomeruli and in damaged proximal tubules. J. Pathol. 148, 55–60.

Huet, G., Hennebicq-Reig, S., de Bolos, C., Ulloa, F., Lesuffleur, T., Barbat, A., Carriere, V., Kim, I., Real, F.X., Delannoy, P., et al. (1998). GalNAc-α-O-benzyl inhibits NeuAcα2-3 glycosylation and blocks the intracellular transport of apical glycoproteins and mucus in differentiated HT-29 cells. J. Cell Biol. 141, 1311–1322.

Jacob, R. and Naim, H.Y. (2001). Apical membrane proteins are transported in distinct vesicular carriers. Curr. Biol. 11, 1444–1450.

Kinlough, C.L., Poland, P.A., Bruns, J.B., Harkleroad, K.L., and Hughey, R.P. (2004). MUC1 membrane trafficking is modulated by multiple interactions. J. Biol. Chem. 279, 53071–53077.

Kinlough, C.L., McMahan, R.J., Poland, P.A., Bruns, J.B., Harkleroad, K.L., Stremple, R.J., Kashlan, O.B., Weixel, K.M., Weisz, O.A., and Hughey, R.P. (2006). MUC1 recycling is dependent on its palmitoylation. J. Biol. Chem. 281, 12112–12122.

Li, Y., Ren, J., Yu, W., Li, Q., Kuwahara, H., Yin, L., Carraway, K.L.I., and Kufe, D. (2001). The epidermal growth factor receptor regulates interaction of the human DF3/MUC1

carcinoma antigen with c-Src and β-catenin. J. Biol. Chem. *276*, 35239–35242.

Ligtenberg, M.J.L., Kruijshaar, L., Buijs, F., van Meijer, M., Litvinov, S.V., and Hilkens, J. (1992). Cell-associated episialin is a complex containing two proteins derived from a common precursor. J. Biol. Chem. *267*, 6171–6177.

Lillehoj, E.P., Kim, B.T., and Kim, K.C. (2002). Identification of Pseudomonas aeruginosa flagellin as an adhesin for Muc1 mucin. Am. J. Physiol. Lung Cell. Mol. Physiol. *282*, L751–L756.

Litvinov, S.V. and Hilkens, J. (1993). The epithelial sialomucin, episialin, is sialylated during recycling. J. Biol. Chem. *268*, 21364–21371.

Macao, B., Johansson, D.G., Hansson, G.C., and Hard, T. (2006). Autoproteolysis coupled to protein folding in the SEA domain of the membrane-bound MUC1 mucin. Nat. Struct. Mol. Biol. *13*, 71–76.

Muller, L., Barret, A., Picart, R., and Tougard, C. (1997). Proteolytic processing of sulfated secretogranin II in the trans-Golgi network of GH3B6 prolactin cells. J. Biol. Chem. *272*, 3669–3673.

Nakatsukasa, K. and Brodsky, J.L. (2008). The recognition and retrotranslocation of misfolded proteins from the endoplasmic reticulum. Traffic *9*, 861–870.

Parry, S., Silverman, H.S., McDermott, K., Willis, A., Hollingsworth, M.A., and Harris, A. (2001). Identification of MUC1 proteolytic cleavage sites *in vivo*. Biochem. Biophys. Res. Commun. *283*, 715–720.

Peat, N., Gendler, S.J., Lalani, N., Duhig, T., and Taylor-Papadimitriou, J. (1992). Tissue-specific expression of a human polymorphic epithelial mucin (MUC1) in transgenic mice. Cancer Res. *52*, 1954–1960.

Pemberton, L.F., Rughetti, A., Taylor-Papadimitriou, J., and Gendler, S.J. (1996). The epithelial mucin MUC1 contains at least two discrete signals specifying membrane localization in cells. J. Biol. Chem. *271*, 2332–2340.

Pochampalli, M.R., Bejjani, R.M., and Schroeder, J.A. (2006). MUC1 is a novel regulator of ErbB1 receptor trafficking. Oncogene *26*, 1693–1701.

Polishchuk, R., Di Pentima, A., and Lippincott-Schwartz, J. (2004). Delivery of raft-associated, GPI-anchored proteins to the apical surface of polarized MDCK cells by a transcytotic pathway. Nat. Cell Biol. *6*, 297–307.

Potter, B.A., Hughey, R.P., and Weisz, O.A. (2006). Role of N- and O-glycans in polarized biosynthetic sorting. Am. J. Physiol. Cell Physiol. *290*, C1–C10.

Ramasamy, S., Duraisamy, S., Barbashov, S., Kawano, T., Kharbanda, S., and Kufe, D. (2007). The MUC1 and galectin-3 oncoproteins function in a microRNA-dependent regulatory loop. Mol. Cell *27*, 992–1004.

Singh, P.K. and Hollingsworth, M.A. (2006). Cell surface-associated mucins in signal transduction. Trends Cell Biol. *16*, 467–476.

Zotter, S., Hageman, P.C., Lossnitzer, A., Mooi, W.J., and Hilgers, J. (1988). Tissue and tumor distribution of human polymorphic epithelial mucin. Cancer Rev. *11–12*, 55–101.